Journal of Process Control 50 (2017) 56–65

Contents lists available at ScienceDirect

Journal of Process Control

journal homepage: www.elsevier.com/locate/jprocont

An integral approach to inferential quality control with self-validating soft-sensors

José L. Godoy[a,b,*], Jacinto L. Marchetti[a], Jorge R. Vega[a,c]

[a] INTEC (CONICET and Universidad Nacional del Litoral), Güemes 3450, 3000, Santa Fe, Argentina
[b] FRP-UTN (Facultad Regional Paraná – Universidad Tecnológica Nacional), Av. Almafuerte 1033, 3100, Paraná, Argentina
[c] FRSF-UTN (Facultad Regional Santa Fe – Universidad Tecnológica Nacional), Lavaisse 610, 3000, Santa Fe, Argentina

ARTICLE INFO

Article history:
Received 16 July 2015
Received in revised form 20 July 2016
Accepted 2 December 2016
Available online 23 December 2016

Keywords:
Integral design space
Multivariate quality control
Partial least squares
Self-validating soft-sensor
Fault detection and diagnosis
Styrene-butadiene rubber (SBR)

ABSTRACT

This paper presents an integral technique for designing an inferential quality control applicable to multivariate processes. The technique includes a self-validating soft-sensor and a multivariate quality control index that depends on the specifications. Based on a partial least squares (PLS) decomposition of the online process measurements, a fault detection and diagnosis technique is used to develop an improved self-validation strategy that is able to confirm, correct or reject the soft-sensor predictions. Model extrapolations, disturbances or sensor faults are first detected through a combined statistic (that considers the calibration region); then, a diagnosis is made by combining statistics pattern recognition, contribution analysis, and disturbance isolation based on historical fault patterns. An off-spec alarm is produced when the proposed index detects that an operating point lies outside the integral design space driven by the specifications. The effectiveness of the proposed technique is evaluated by means of two numerical examples. First, a synthetic example is used to interpret the fundamentals of the method. Then, the technique is applied to the industrial Styrene-Butadiene rubber process, which is emulated through an available numerical simulator.

1. Introduction

In most industrial processes, the automatic control systems (or even the operators) adjust the manipulated variables with the aim of fulfilling several goals, e.g. to maintain the product quality within specifications, to limit the waste or contaminating emissions according to government regulations, and to keep the process close to an optimal operation condition that is normally established from both economical and technical point of views. An adequate driving of the manipulated variables is clearly conditioned to the availability of accurate and fast measurements. Typically, the process measurements are available from either online analyzers or offline laboratory equipments. Unfortunately, many important process variables cannot accurately be measured in relatively short times, thus negatively affecting real-time control strategies. In such cases, soft-sensors can help to overcome the problem. A soft-sensor is a mathematical code able to infer some unmeasured variables from a set of online measured variables. In the last years, soft-sensor applications have brought significant attention in the process industry [1–5]. In particular, several techniques based on partial least squares (PLS) have been used for monitoring complex industrial processes where the quality variables are important [6,7].

The efficiency of a soft-sensor as a predictive tool depends on several factors, such as: i) the accuracy of the process model that was used to derive the soft-sensor; ii) the proper adjustment of the soft-sensor to the actual process operating point; and iii) the availability of adequate online measurements. In general, process disturbances and sensor faults can strongly modify the correlated measurements, and therefore the quality predictions become unreliable. To overcome these difficulties, several strategies have been reported in the literature [8,9]. For example, Liu et al. [8] proposed a PLS-based soft-sensor with self-validation and reconstruction of faulty readings that improve the reliability of the predictions. The strategy consisted in an initial validation of the measurements prior to predicting the quality variables through the soft-sensor. The detection of a faulty sensor was followed by a reconstruction of the corresponding faulty readings; however, the identification of the faulty sensors was not fully reliable [8,10].

A fault detection and diagnosis strategy applicable to multivariate processes typically includes three main tasks: 1) the detection of an anomaly or an out-of-control condition; 2) the classification

* Corresponding author at: INTEC (CONICET and Universidad Nacional del Litoral), Güemes 3450, Santa Fe, 3000, Argentina.
E-mail address: jlgodoy@santafe-conicet.gov.ar (J.L. Godoy).

http://dx.doi.org/10.1016/j.jprocont.2016.12.001
0959-1524/

of the fault that generated the abnormal behavior, and 3) the isolation of the disturbed variables and ideally of the disturbing sources. Godoy et al. [11] proposed a PLS-based fault detection and diagnosis technique for multivariate processes that assumes available online measurements of the quality variables. According to such approach, the projections of the process measurements onto the latent space induce a PLS-decomposition of such measurements into four non-overlapped subspaces, and then, a combined index can be used to detect the process anomalies. The technique allows for an efficient anomaly classification as well as the identification of the disturbed variables. The pattern of the statistics that compose the detection index can be used to classify the anomaly type. However, no specification-dependent control limits were included for those statistics, as it is normally required for establishing quality control strategies.

Contribution plots are tools typically used for the identification of sources of faults without requiring any prior fault information [7,10]. On the basis of a principal component analysis (PCA) model, Alcala and Qin [12] have proposed a reconstruction-based contribution (RBC) technique to diagnose process faults. This technique inherits the merit of traditional contribution plots and has a solid theoretical foundation for detecting faulty sensors without smearing problems. However, RBC is only useful to isolate those failed sensors that do not cause the fault propagation to other variables, while it is ineffective for complex faults such as process faults and disturbances [10]. On the other hand, the angle between the vectors corresponding to the measurements and the fault signatures has been used to isolate complex faults [2,13]. Generalized RBCs based on fault subspaces have also been used to isolate know process faults [14], but need several faulty samples for extracting each fault subspace. In contrast, the angular measures have the advantage of only requiring a single faulty sample of each know fault to implement the diagnosis stage. It has been proven that the diagnosis results are the same for both approaches, because the ratio "generalized RBCs/detection index" is equal to the angular measure given by the squared cosine of the angle between the current PCA-projection and the faulty PCA-projection [10].

The role of design spaces (or multivariate specification regions) is undoubtedly important in several processes, and aims at reducing statistical variations in the final product quality by design rather than by inspection. The International Conference on Harmonization Q8 (ICH-Q8) document [15] defines a design space as "the multidimensional combination and interaction of input variables (e.g., material attributes) and process parameters that have been demonstrated to provide assurance of quality." The current trend is towards defining multivariate specifications in the low dimensional subspace defined by a PLS model [16,17]. An integral design space should include a quality driven specification for the raw materials to be used in the process under certain operating conditions. Such specification will have to account for the inherent variability in the process and the combined effect of incoming materials with process conditions onto product quality [18].

Control of industrial polymerization processes is difficult due to the lack of sensor devices capable of providing with accurate online measurement of most quality variables [19]. Currently, there are several applications of soft-sensors in polymerization processes (e.g., Gonzaga et al. [20]). In particular, Godoy et al. [21] have developed a PLS soft-sensor capable of monitoring the production of Styrene-Butadiene rubber (SBR) in an industrial train of 7 continuously-stirred tank reactors. However, the presence of disturbances or sensor faults can turn unreliable the soft-sensor predictions.

In this work, an integral technique for inferential quality control is presented. To this effect, a PLS model is used to define an integral design space driven by quality specifications that accounts for the relationships between incoming materials, process conditions and product quality. Based on this integral design space, a statistical index is proposed for quality control. Additionally, this work presents a self-validation strategy for the inferences provided by a soft-sensor that estimates quality variables in a multivariate process (see Fig. 1). Such strategy is based on a fault detection and diagnosis method previously designed for processes with online measurable outputs [11], and includes: i) an extrapolation control limit, ii) pattern analysis of the statistics that compose a fault detection index, iii) RBC analysis for the identification of the contributing variables or faulty sensors, and iv) a disturbance isolation method based on the angle differences between current measurements and the historical disturbances. The proposed self-validation strategy contributes to improve the soft-sensor inferences by adding a procedure able to alarm the presence of extrapolations, disturbances or sensor faults, and to eventually correct faulty readings. The effectiveness of the proposed integral technique for inferential quality control is first demonstrated through a numerical example. Then, a self-validation strategy is developed for the simulator of an industrial SBR process; and in such a sense, the present work extends the applicability of the soft-sensor developed by Godoy et al. [21].

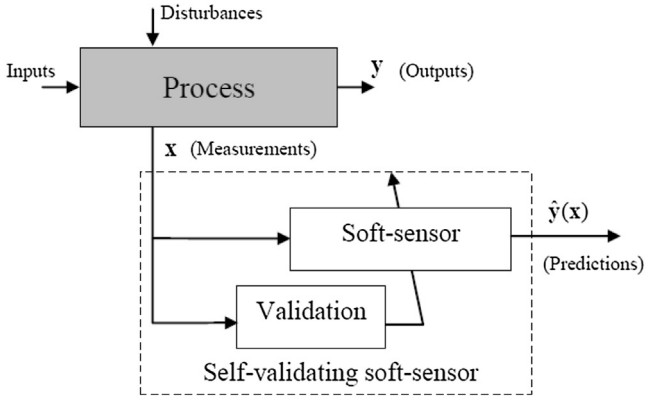

Fig 1. Inferential quality control with a self-validating soft-sensor. The soft-sensor predictions ($\hat{\mathbf{y}}$) are confirmed, corrected, or rejected by the proposed validation strategy.

2. Inferential quality control with self-validating soft-sensor

For a given multivariate process, call $\mathbf{x} = [x_1 \ldots x_m]' \in \Re^m$ the vector of online measurements and $\mathbf{y} = [y_1 \ldots y_p]' \in \Re^p$ the vector of quality variables. Both $\mathbf{x}$ and $\mathbf{y}$ are standardized vectors (i.e., mean-centered and scaled). Assume that N offline measurements of each variable were collected while the process was operating under normal conditions. Then, the following extended PLS regression model can be derived [11]:

$$\mathbf{x} = \mathbf{Pt} + \tilde{\mathbf{x}}, \mathbf{y} = \mathbf{Qu} + \tilde{\mathbf{y}}, \quad (1)$$

$$\mathbf{u} = \mathbf{Bt} + \tilde{\mathbf{u}}, \quad (2)$$

where $\{\tilde{\mathbf{x}}, \tilde{\mathbf{y}}, \tilde{\mathbf{u}}\}$ are the model residuals, and the latent vectors $\mathbf{t}$ and $\mathbf{u}$ are respectively calculated from $\mathbf{x}$ and $\mathbf{y}$, as follows:

$$\mathbf{t} = \mathbf{R}'\mathbf{x}, \mathbf{u} = \mathbf{S}'\mathbf{y}. \quad (3)$$

The matrices $\mathbf{P}$, $\mathbf{Q}$, $\mathbf{R}$, $\mathbf{S}$, and $\mathbf{B}$, are obtained through the PLS-NIPALS algorithm [11,22,23]. This technique implicitly assumes that both $\mathbf{x}$ and $\mathbf{y}$ are online measured, and projects the measurement vectors into low-dimension spaces defined by A latent variables which are then regressed.

In this work we assume that the quality variables, $\mathbf{y}$, are not online available. On the basis of Eqs. (1), (2) and (3), it is possible to

predict $\mathbf{y}$ from the current measurements $\mathbf{x}$, through the following inferential model (or soft-sensor):

$$\hat{\mathbf{y}} = \mathbf{QBt} = \mathbf{QBR}'\mathbf{x} \in S_{MY}, \tag{4}$$

where S_{MY} is the output model subspace. The multivariate specification region (or *design space*) for the product quality is given by: $\mathbf{y}_{\min} \le \mathbf{y} \le \mathbf{y}_{\max}$, where $\mathbf{y}_{\min}$ and $\mathbf{y}_{\max}$ are the standardized specification limits. Then, the product quality is assumed in-control provided that: $\mathbf{y}_{\min} + \boldsymbol{\varepsilon}_y \le \hat{\mathbf{y}} \le \mathbf{y}_{\max} - \boldsymbol{\varepsilon}_y$, where $\boldsymbol{\varepsilon}_y$ is the standard calibration error.

2.1. Multivariate quality control index

The geometric intersection of the specification region with the output model subspace S_{MY} (spanned by $\mathbf{Q}$) determines the effective specification region (or integral design space), given by the following polytope in $\mathbf{u}$:

$$P = \{\mathbf{u} : \mathbf{Au} \le \mathbf{b}\}, \tag{5.a}$$

with

$$\overbrace{\begin{bmatrix}\mathbf{I}\\ -\mathbf{I}\end{bmatrix}}^{\mathbf{A}}\mathbf{Qu} \le \overbrace{\begin{bmatrix}\mathbf{y}_{\max} - \boldsymbol{\varepsilon}_y\\ -\mathbf{y}_{\min} - \boldsymbol{\varepsilon}_y\end{bmatrix}}^{\mathbf{b}}. \tag{5.b}$$

The integral design space in the process variables $\mathbf{x}$ (or the region where the variables $\mathbf{x}$ are acceptable), isthe mapping of the $\mathbf{y}$-region back into the $\mathbf{x}$-space, i.e.: $\mathbf{ABR}'\mathbf{x} \le \mathbf{b}$ (see Eq. (5)). Then, the (squared) distance from a given projected point $\hat{\mathbf{u}} = \mathbf{BR}'\mathbf{x}$ to the set P, is defined as the minimum distance between the point and every element in the set, i.e.:

$$d(\hat{\mathbf{u}}, P) = \min_{\mathbf{u} \in P}\left(\|\hat{\mathbf{u}} - \mathbf{u}\|^2\right), \tag{6}$$

where $\hat{\mathbf{u}} = \mathbf{Bt} = \mathbf{BR}'\mathbf{x}$ is the prediction of $\mathbf{u}$ (see Eqs. (2) and (3)) and $d(\hat{\mathbf{u}}, P) = 0$ for $\hat{\mathbf{u}} \in P$. The simultaneous assessment index (Eq. (6)) is proposed for accepting/rejecting the incoming materials and process conditions given in $\mathbf{x}$.

2.2. Multivariate capability index

It has been proven [11] that the Mahalanobis distances computed from $\hat{\mathbf{x}}$, $\mathbf{t}$, $\hat{\mathbf{u}}$, and $\hat{\mathbf{y}}$ are equivalent, i.e. $D_{\hat{\mathbf{x}}} = T^2_{\mathbf{t}} = T^2_{\hat{\mathbf{u}}} = D_{\hat{\mathbf{y}}}$. In particular, the Mahalanobis distance of $\mathbf{t}$ ($T^2_{\mathbf{t}} = \mathbf{t}'\boldsymbol{\Lambda}^{-1}\mathbf{t}$) is equivalent to the generalized Mahalanobis distance of $\hat{\mathbf{y}}$ $\left(D_{\hat{\mathbf{y}}} = \hat{\mathbf{y}}'\mathbf{R}^-_{\hat{\mathbf{y}}}\hat{\mathbf{y}}\right)$, and in combination with Eq. (3) one has:

$$T^2_{\mathbf{t}} = \mathbf{x}'\mathbf{R}\boldsymbol{\Lambda}^{-1}\mathbf{R}'\mathbf{x} = \hat{\mathbf{u}}'\boldsymbol{\Delta}^{-1}\hat{\mathbf{u}} = \hat{\mathbf{y}}'\mathbf{R}^-_{\hat{\mathbf{y}}}\hat{\mathbf{y}} = D_{\hat{\mathbf{y}}} \tag{7}$$

where $\mathbf{R}_{\hat{\mathbf{y}}} = \mathbf{Q}\boldsymbol{\Delta}\mathbf{Q}'$ is the correlation matrix of $\hat{\mathbf{y}}$, $\boldsymbol{\Delta} = \mathbf{B}\boldsymbol{\Lambda}\mathbf{B}$ is the correlation matrix of $\hat{\mathbf{u}}$, and $\boldsymbol{\Lambda} = diag(\lambda_1 \ldots \lambda_A)$ is the correlation matrix of $\mathbf{t} = [t_1 \cdots t_A]'$. Eq. (7) suggests that the behaviour of $\mathbf{y}$ can be monitored from the available measurements $\mathbf{x}$, i.e. the deviation of the predicted quality vector $\hat{\mathbf{y}}$ can be measured through $T^2_{\hat{\mathbf{u}}} = \hat{\mathbf{u}}'\boldsymbol{\Delta}^{-1}\hat{\mathbf{u}}$. Then, for inferential quality control, such measure can be compared to a limit that depends on the specifications.

A multivariate control limit modified by the specifications can be defined as the K^2 constant density contour with generating matrix $\boldsymbol{\Delta}$ (i.e., $\mathbf{u}'\boldsymbol{\Delta}^{-1}\mathbf{u} = K^2$) and with the greatest volume entirely contained inside the effective specification region P, described by Eq. (5). The volume of the ellipsoid $E = \left\{\mathbf{u} = K\boldsymbol{\Delta}^{1/2}\mathbf{z} : \|\mathbf{z}\| \le 1\right\}$ is given by: $vol(E) = |K^2\boldsymbol{\Delta}|^{1/2}\pi^{A/2}/\Gamma(A/2+1)$, where Γ is the Gamma function. Thus, $\log vol(E) = 1/2\log|K^2\boldsymbol{\Delta}| + \text{constant}$. Hence, the K^2 control limit can be computed by means of the following convex optimization problem in K [24]:

$$\begin{aligned}
&\max \log vol(E) \quad \equiv \quad \max \log(K)\\
&s.t.\ \ E \subseteq P \qquad\quad s.t. \quad K > 0,\\
&\qquad\qquad\quad \|K\boldsymbol{\Delta}^{1/2}\mathbf{a}_i\| \le \mathbf{b}(i), \quad i = 1, \ldots, 2p\\
&\qquad\quad \equiv \min \log(1/K)\\
&\qquad\quad\ s.t. \quad K > 0,\\
&\qquad\qquad\quad K^2\mathbf{a}'_i\boldsymbol{\Delta}\mathbf{a}_i \le \mathbf{b}(i)^2, \quad i = 1, \ldots, 2p
\end{aligned} \tag{8}$$

where $\mathbf{a}'_i$ is i-th row of $\mathbf{A}$ and $\mathbf{b}(i)$ is the i-th element of $\mathbf{b}$ (see Eq. (5)). Then, a multivariate capability index (MC_P) can be defined as the ratio of the effective tolerance region volume to the process region volume, i.e.:

$$MC_P = \frac{vol\left(\mathbf{u}'\boldsymbol{\Delta}^{-1}\mathbf{u} \le K^2\right)}{vol\left(\mathbf{u}'\boldsymbol{\Delta}^{-1}\mathbf{u} \le \tau^2_\alpha\right)} = \left(\frac{K^2}{\tau^2_\alpha}\right)^{A/2}, \tag{9}$$

where the numerator is an ellipsoidal volume given by: $\left(K^2\right)^{A/2}|\boldsymbol{\Delta}|^{1/2}\pi^{A/2}/\Gamma(A/2+1)$, and τ^2_α is the confidence limit of the $T^2_{\mathbf{u}}$ statistic. The process will be accepted as capable when $MC_P \ge 1$.

2.3. Validation of the predictions

The predictive ability of the inferential model of Eq. (4) depends on both the plant-model match and the quality of the current measurements, $\mathbf{x}$. In this approach, both the measurements and the process will be checked by means of a fault detection index that is computed prior to validate the prediction of $\mathbf{y}$.

For new data $\mathbf{x}$, the prediction uncertainty of the PLS model (Eq. (4)) is related to both $T^2_{\mathbf{t}}$ and the calibration region (that covers the calibration data). To perform a reliable test of extrapolation, the region covered by the calibration data in the model subspace is first determined. The ellipsoid of minimum volume $E = \left\{\mathbf{t} : \mathbf{t}'\boldsymbol{\Lambda}^{-1}\mathbf{t}/\rho^2 \le 1\right\}$ that contains the projected calibration points $\mathbf{t}_i = \mathbf{R}'\mathbf{x}_i$ ($i = 1, \ldots, N$) can be computed by solving the following convex problem [24]:

$$\begin{aligned}
&\min \log(\rho)\\
&s.t. \quad \rho > 0,\\
&\quad \|\rho^{-1}\boldsymbol{\Lambda}^{-1/2}\mathbf{t}_i\| \le 1, \quad i = 1, \ldots, N.
\end{aligned} \tag{10}$$

Then, the ρ^2 density contour of $T^2_{\mathbf{t}}$ can be used for extrapolation testing. A value $T^2_{\mathbf{t}}/\rho^2 > 1$ suggests that at least one $\mathbf{x}$-variable lies out of the calibration region. Therefore, the use of ρ^2 (instead of τ^2_α) improves the reliability of the extrapolation test.

The PLS model induces the following decomposition of the sampled data, $\mathbf{x}$ [11]:

$$\mathbf{x} = \hat{\mathbf{x}} + \tilde{\mathbf{x}} \in \Re^m, \ \hat{\mathbf{x}} = \mathbf{PR}'\mathbf{x} \in S_{MX}, \ \tilde{\mathbf{x}} = \left(\mathbf{I} - \mathbf{PR}'\right)\mathbf{x} \in S_{RX}, \tag{11}$$

where $\hat{\mathbf{x}}$ is the oblique projection of $\mathbf{x}$ onto the model subspace S_{MX} along residual subspace S_{RX}, and $\tilde{\mathbf{x}}$ is the oblique projection of $\mathbf{x}$ onto S_{RX} along S_{MX}. Note that $\hat{\mathbf{x}}$ can also be written as $\hat{\mathbf{x}} = \mathbf{Pt}$.

For a process with online measurable $\mathbf{x}$ and $\mathbf{y}$ variables, one can define a combined index able to efficiently monitor the whole measurement space, with a reduced probability of both false alarms and undetected faults. This combined index is a balanced merging of several scaled metrics that includes a Mahalanobis distance for considering the process correlations and three Euclidean distances to the correlations model.

When the process outputs **y** are unavailable online, then the combined index established by Godoy et al. [11] must be restricted to only include the online measurements, **x**; i.e.:

$$I_C(\mathbf{x}) = \frac{T_{\mathbf{t}}^2}{\rho^2} + \frac{SPE_{\mathbf{x}}}{\delta^2_{\mathbf{x},\,\alpha}} = I_{MX}(\mathbf{x}) + I_{RX}(\mathbf{x}) = \mathbf{x}'\boldsymbol{\Phi}\mathbf{x}\,, \tag{12.a}$$

with

$$\boldsymbol{\Phi} = \frac{1}{\rho^2}\mathbf{R}\boldsymbol{\Lambda}^{-1}\mathbf{R}' + \frac{1}{\delta^2_{\mathbf{x},\,\alpha}}\left(\mathbf{I} - \mathbf{P}\mathbf{R}'\right)'\left(\mathbf{I} - \mathbf{P}\mathbf{R}'\right)\,, \tag{12.b}$$

where $\boldsymbol{\Phi}$ is a symmetric positive-definite matrix, $SPE_{\mathbf{x}}$ is the squared prediction error (SPE), and $\delta^2_{\mathbf{x},\,\alpha}$ is the confidence limit of the SPE statistic. The index defined in Eq. (12) differs from the original one in the scale of $T^2_{\mathbf{t}}$ [11]; in fact, the original confidence limit τ^2_α has been replaced by the model extrapolation limit ρ^2. Note that I_C simultaneously considers the entire input space $\Re^m = S_{MX} + S_{RX}$ and the output model subspace S_{MY}. For this reason, we propose the use of the I_C index to develop a self-validating strategy able to confirm (or reject) the soft-sensor predictions (Eq. (4)). The control limit (at confidence level α), I_α, is estimated via the kernel density estimation (KDE) approach [25–27]. The inferential model of Eq. (4) is positively validated when $I_C < I_\alpha$, while the predictions are no longer reliable when $I_C \geq I_\alpha$. In this last case, it is necessary to diagnose the anomaly type that is present in the process (an extrapolation or an abnormality). I_{MX} and I_{RX} (in Eq. (12)) are the normalized statistics that compose I_C and measure variations in S_{MX} and S_{RX}, respectively; then the potential extrapolation can be monitored through I_{MX} while the sensor faults and the process abnormalities are monitored through I_{RX}.

An alternative approach for validating predictions of a soft-sensor has been used by Liu et al. [8], by adding confidence intervals (CIs) to the PLS-predictions to ensure the reliability of the incoming measurements **x**. In absolute units, the uncertainty in the j-th prediction corresponding to a new sample **x** was calculated as [8]:

$$\begin{aligned}\hat{\sigma}^2\left(y_j - \hat{y}_j\right) &= \hat{\sigma}^2\left(y_j\right)\left[1 + \mathbf{x}'\mathbf{R}\boldsymbol{\Lambda}^{-1}\mathbf{R}'\mathbf{x}/(N-1)\right] \\ &= \hat{\sigma}^2\left(y_j\right)\left[1 + T^2_{\mathbf{t}}/(N-1)\right]\end{aligned} \tag{13}$$

where $\hat{\sigma}^2(y_j)$ is the y_j-variance estimated in the set of N samples collected. Then, the $(1-\alpha)$ CI of the new j-th prediction through the PLS model is given by: $CI_j = \pm t_{\alpha/2,N-m}\hat{\sigma}(y_j - \hat{y}_j)$, where $t_{\alpha/2,N-m}$ is a t-distribution with N-m degrees of freedom. Hence, Eq. (4) is not suitable for predictions outside the CIs, i.e. when $\hat{y}_j^2 > t^2_{\alpha/2,N-m}\hat{\sigma}^2(y_j - \hat{y}_j)$ ($j = 1\ldots p$). Note that the CIs depend only on the statistic $T_t{}^2$ in S_{MX} (see Eq. (13)); while the index I_C (Eq. (12)) is a complete measure of variability in **x**, which simultaneously consider both subspaces S_{MX} and S_{RX}. Also, for a well-adjusted PLS model, the sensor faults and disturbances mainly affect S_{RX} [11]. In principle, the I_C-based validation would be more reliable than the approach based on CIs. Also, the I_C-based validation would be more reliable than the monitoring method by Masuda et al. [9]. This last method includes the soft-sensor predictions in the fault detection strategy, but such predictions do not add new information (see Eq. (7)).

2.3.1. Abnormality diagnosis

The diagnosis method proposed in this work combines statistics pattern recognition, contribution analysis, and disturbance isolation. Godoy et al. [11] established that: i) the process upset points are characterized by high I_{MX} and negligible I_{RX}, ii) correlation changes (or disturbances) and sensor faults are characterized by negligible I_{MX} and high I_{RX}, and iii) sensor faults can be distinguished from correlation changes through an appropriate contribution analysis.

Fig. 2 shows the proposed validation strategy. In the normal case, i.e. when $I_C(\mathbf{x}) < I_\alpha$, the soft-sensor predictions are automatically validated. By contrast, an abnormality is first detected when $I_C(\mathbf{x}) \geq I_\alpha$; and then it is classified on the basis of I_{MX} and I_{RX} contribution patterns as: i) a model extrapolation (type 1), ii) a sensor fault (type 2), or iii) a correlation change (type 3). According to the resulting type, the process upset, the faulty sensor or the incoming disturbance must be identified. An abnormality of type 1 indicates a low predictive capability due to a model extrapolation, and therefore the predictions are not fully reliable. In particular, an abnormality of type 2 can be compensated by a proper reconstruction of the faulty reading. In contrast, an abnormality of type 3 indicates a low predictive capability due to a plant-model mismatch; as a consequence, the soft-sensor predictions are not fully reliable and the incoming disturbance should be identified through some independent procedure.

Consider the case of a fault classified as type 2. First, the faulty sensor is identified by contribution analysis (see Section 2.3.1.1). Then, the true reading of the faulty sensor can be reconstructed from the remaining reliable readings, as follows [8]:

$$\mathbf{x}^r = \mathbf{x}^r_f + (\mathbf{I} - diag(\boldsymbol{\xi}))\mathbf{x}, \tag{14}$$

with

$$\mathbf{x}^r_f = -((\mathbf{I} - diag(\boldsymbol{\xi}))\boldsymbol{\Phi})^-(\mathbf{I} - diag(\boldsymbol{\xi}))\boldsymbol{\Phi}(\mathbf{I} - diag(\boldsymbol{\xi}))\mathbf{x},$$

where $diag(\boldsymbol{\xi})$ is a diagonal matrix with elements equal to one for the faulty sensors and zero for normal sensors. Then, the **y**-prediction (Eq. (4)) is performed without the influence of the faulty readings using $\mathbf{x}^r$. The reconstruction of Eq. (14) attenuates the disturbing effect of wrong measurements on the model predictions.

2.3.1.1. Contribution analysis for isolating faulty sensors.

Contribution plots are frequently used to isolate the detected faulty variables without using historical fault patterns [10]. In this work, the RBC was adopted due to its diagnostic reliability when $\boldsymbol{\Phi} > 0$ (see Eq. (12)) [10,12]. In a process with m sensors, the fault direction in the i-th sensor is described by $\boldsymbol{\xi}_i = [0\cdots1\cdots0]' \in R^m$ (i.e., zeros entries except for the i-th location that takes a unitary value). Then, the contribution of the wrong measurement x_i to the fault detection index I_C, RBC_i, is the amount of reconstruction along $\boldsymbol{\xi}_i$, given by [12]:

$$RBC_i = (f_i\,\boldsymbol{\xi}_i)'\boldsymbol{\Phi}(f_i\,\boldsymbol{\xi}_i) = \frac{\left(\boldsymbol{\xi}'_i\boldsymbol{\Phi}\mathbf{x}\right)^2}{\boldsymbol{\xi}'_i\boldsymbol{\Phi}\boldsymbol{\xi}_i}\,, \tag{15}$$

where $f_i = \left(\boldsymbol{\xi}'_i\boldsymbol{\Phi}\boldsymbol{\xi}_i\right)^{-1}\left(\boldsymbol{\xi}'_i\boldsymbol{\Phi}\mathbf{x}\right)$ is the magnitude of the fault and $I_C(\mathbf{x}) = I_C(\mathbf{x} - f_i\boldsymbol{\xi}_i) + RBC_i$. Even in the absence of faults, the RBCs of the sensors are different. Then, it is advisable to use a control limit for each RBC_i, as given by [12]: $\delta_i = \left(\boldsymbol{\xi}'_i\boldsymbol{\Phi}\mathbf{R}_{\mathbf{x}}\boldsymbol{\Phi}\boldsymbol{\xi}_i\right)\left(\boldsymbol{\xi}'_i\boldsymbol{\Phi}\boldsymbol{\xi}_i\right)^{-1}\chi^2_\alpha(1)$ ($i = 1\ldots m$). A fault in the i-th sensor ($f_i\boldsymbol{\xi}_i$) does not propagate to other measurements, thus a significant RBC_i directly identifies the faulty sensor. By contrast, a disturbance can propagate to other variables by affecting the correlation pattern of **x**. This effect induces several significant contributions that prevent a direct isolation of the root cause.

2.3.1.2. Disturbance isolation.

Consider in what follows a graphical interpretation of a disturbed measurement **x** (or anomaly Type 3). In such case, **x** deviates from the model subspace S_{MX}, and the angles between **x** and the oblique

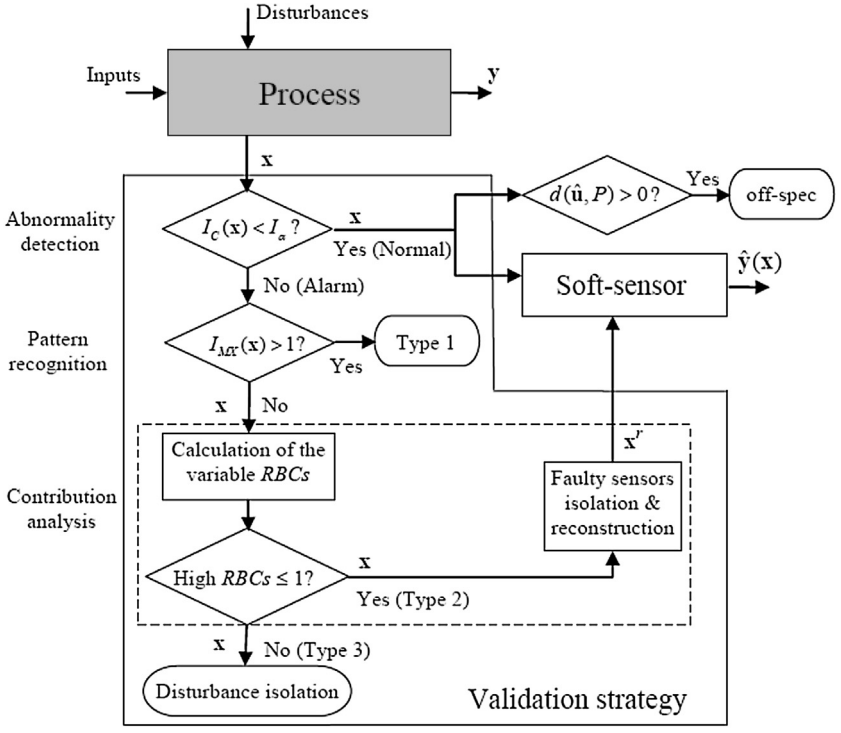

Fig. 2. The proposed validation strategy.

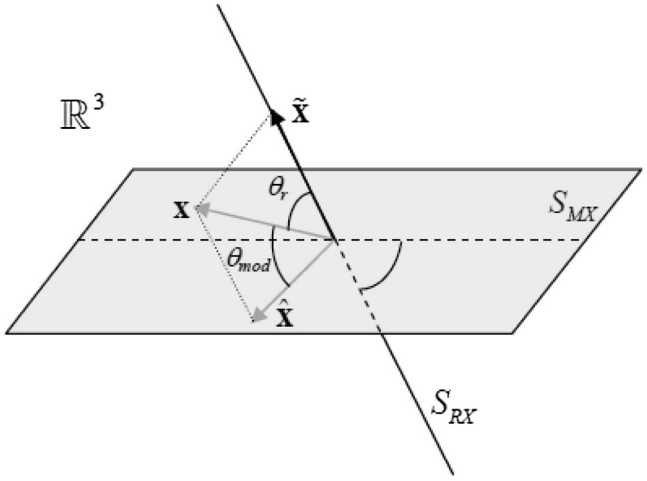

Fig. 3. PLS-decomposition of the measurement vector **x** in two oblique subspaces (S_{MX} and S_{RX}). The angles θ_{mod} and θ_r can be used to characterize the disturbance.

subspaces S_{MX} and S_{RX} could be used to characterize the event (see Fig. 3). Such angles are calculated as follows:

$$\theta_{\text{mod}} = \cos^{-1}\left(\hat{\mathbf{x}}'\mathbf{x}/\|\hat{\mathbf{x}}\|\|\mathbf{x}\|\right), \quad \theta_r = \cos^{-1}\left(\tilde{\mathbf{x}}'\mathbf{x}/\|\tilde{\mathbf{x}}\|\|\mathbf{x}\|\right), \tag{16}$$

where the projections of **x** onto the model and residual subspaces ($\hat{\mathbf{x}}$ and $\tilde{\mathbf{x}}$, respectively) are oblique, i.e.: $\hat{\mathbf{x}}'\tilde{\mathbf{x}} \neq 0$ (or $\theta_{\text{mod}} + \theta_r \neq 90^\circ$).

We propose to isolate the disturbances on the basis of the angular measures. More specifically, we will use the cosine of the angle between a current projection $\hat{\mathbf{x}}$ ($\tilde{\mathbf{x}}$) and a known abnormal projection $\hat{\mathbf{x}}_i$ ($\tilde{\mathbf{x}}_i$); i.e., $\cos\hat{\theta}_i = \left(\hat{\mathbf{x}}'\hat{\mathbf{x}}_i\right)/\|\hat{\mathbf{x}}\|\|\hat{\mathbf{x}}_i\|$ ($\cos\tilde{\theta}_i = \left(\tilde{\mathbf{x}}'\tilde{\mathbf{x}}_i\right)/\|\tilde{\mathbf{x}}\|\|\tilde{\mathbf{x}}_i\|$), where $\{\hat{\mathbf{x}}_i \in S_{MX}\}_{i=1,\ldots,l}$ and $\{\tilde{\mathbf{x}}_i \in S_{RX}\}_{i=1,\ldots,l}$ are the l known disturbances projected on both subspaces. Thus, when the absolute value of the i-th cosine is close to one, then the current projection $\hat{\mathbf{x}}$ (or $\tilde{\mathbf{x}}$) tends to be collinear with the i-th abnormal projection $\hat{\mathbf{x}}_i$ (or $\tilde{\mathbf{x}}_i$). Hence, a disturbance can be isolated as follows:

$$i_d = \underset{i=1\ldots l}{arg}\left[\max\left(\cos\hat{\theta}_i \cos\tilde{\theta}_i\right)\right], \quad s.t. \ \ |\cos\hat{\theta}_i| > \eta, \ |\cos\tilde{\theta}_i| > \eta \tag{17}$$

where the threshold $\eta < 1$ restricts the acceptance region to $\pm\cos^{-1}\eta$. This threshold generates conical acceptance regions that are collinear to $\hat{\mathbf{x}}_i$ and $\tilde{\mathbf{x}}_i$ ($i = 1,\ldots,l$).

Note that this method requires a prior knowledge of the set of candidate disturbances. The disturbances samples can be obtained through plant tests, a mechanistic model or historical disturbance data.

If a sensor (involved in **x**) is included in a closed-loop control strategy, then a simple fault originated in such sensor will affect the correlation structure. Therefore, such fault becomes complex [11], and can no longer be identified by contribution analysis. In this case, the proposed disturbance isolation should be used to identify the sensor fault.

3. Simulation examples

Consider in what follows two simulation examples chosen for evaluating the proposed strategy of inferential quality control with self-validating soft-sensor.

3.1. A synthetic example

Consider a hypothetical process with 3 quality attributes arranged into the vector $\mathbf{y}' = [y_1, y_2, y_3]$, which are correlated to 7 process variables arranged into the measurement vector $\mathbf{x}' = [x_1 \ldots$

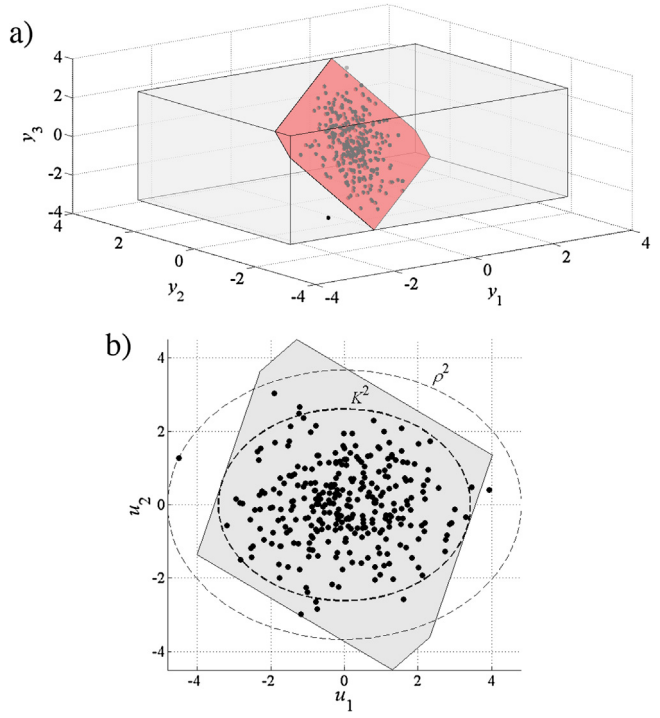

Fig. 4. a) Specification region containing the effective specification region. b) Scatter plot of the projected calibration data, effective specification region containing the maximum volume ellipsoid (K^2 density contour), and ρ^2 density contour for extrapolation testing.

x_7]. The $\mathbf{x}$ and $\mathbf{y}$ vectors were generated according to the following model [28]:

$$\begin{cases} \mathbf{t} \sim N(\mathbf{0}, \boldsymbol{\Lambda}), & \boldsymbol{\Lambda} = diag(1.4, 0.8) \\ \mathbf{u} = \mathbf{t} + \boldsymbol{\varepsilon}_u, & \boldsymbol{\varepsilon}_u \sim N\left(0, 0.005^2 \mathbf{I}_2\right), \\ \mathbf{x} = \mathbf{P}\,\mathbf{t} + \boldsymbol{\varepsilon}_x, & \boldsymbol{\varepsilon}_x \sim N\left(0, 0.01^2 \mathbf{I}_7\right), \\ \mathbf{y} = \mathbf{Q}\,\mathbf{u} + \boldsymbol{\varepsilon}_y, & \boldsymbol{\varepsilon}_y \sim N\left(0, 0.01^2 \mathbf{I}_3\right), \end{cases} \tag{18}$$

with

$$\mathbf{P} = \begin{bmatrix} 0.4045 & 0 \\ 0 & 0.7906 \\ 0.5394 & 0.1581 \\ 0.2697 & -0.1581 \\ 0.1348 & -0.3162 \\ 0 & 0.4743 \\ 0.6742 & 0 \end{bmatrix}, \quad \mathbf{Q} = \begin{bmatrix} 0.8018 & 0.4472 \\ 0.5345 & 0 \\ 0.2673 & -0.8944 \end{bmatrix}.$$

Three hundred samples were generated with Eq. (18) under normal operating conditions (NOC) for calibration of the PLS-based soft-sensor. Such NOC data were then mean-centered and scaled to unit variance, and a PLS model with two latent variables was identified. The following standardized specifications for $\mathbf{y}$ was defined: $-3.5 \le y_1 \le 3.5$, $-2.5 \le y_2 \le 2.5$, $-2.8 \le y_3 \le 2.8$. Fig. 4(a) shows the collected process observations, the standardized specification region, and the PLS-projection plane (S_{MY}) spanned by the columns of $\mathbf{Q}$. The effective specification region is the intersection of the hypercube with S_{MY}. Note that the variability of the calibration dataset can exceed the quality specifications. In the reduced space (u_1, u_2) obtained from $\mathbf{u} = \mathbf{S}'\mathbf{y}$ (see Eq. (3)), Fig. 4(b) shows the largest K^2 (=6.1436) density contour (dashed line) that is contained in the effective specification region. Fig. 4(b) also shows the ρ^2 (=12.0486) density contour covering the calibration points, where $\rho > K$; and hence, some calibration points are outside of the K^2 contour. On the contrary, when $\rho < K$, the specifications must be contracted in order to reach (at least) $\rho = K$. In this case, the new specification limits can be computed by means of the following convex optimization problem:

$$\begin{aligned} &\min \ \ \|\mathbf{s}\|^2 \\ &s.t. \ \ \mathbf{s}(i) \ge 0, \\ &\|\rho\, \boldsymbol{\Delta}^{1/2} \mathbf{a}_i\| \le \mathbf{b}(i) - \mathbf{s}(i), \quad i = 1, \ldots, 2p \end{aligned} \tag{19}$$

where $\mathbf{s}$ represents the shrinking in each specification required to ensure that the calibration region is included in the new specification region.

The simulated abnormal measurements were of the form:

$$\mathbf{x} = \mathbf{x}^* + f\boldsymbol{\xi}, \tag{20}$$

where the sensor fault was featured by its magnitude f and its direction $\boldsymbol{\xi}$, and the fault-free part $\mathbf{x}^*$ was generated according to the model of Eq. (18) or by modifying the correlation pattern. The faulty samples (Eq. (20)) were standardized on the basis of the mean and variance of the NOC data. The hypothetical process was disturbed according to four abnormal scenarios: a) an abnormality of type 2 (or sensor fault) was simulated with $f\boldsymbol{\xi} = [0.1\ 0\ 0\ 0\ 0\ 0\ 0]'$; b) an abnormality of type 3 was simulated by modifying the correlation structure of $\mathbf{x}$ as follows: $\mathbf{x} = (\mathbf{P} + \Delta\mathbf{P})\mathbf{t} + \boldsymbol{\varepsilon}_x$, where $\Delta\mathbf{P}(:, 1) = \mathbf{0}$ and $\Delta\mathbf{P}(:, 2) = [0\ 0.4\ 0\ 0\ -0.1\ 0.2\ -0.2]'$ (see Eq. (18)); c) an abnormality of type 1 was simulated by shifting the average operating point of $\mathbf{t} = [0\ 0]'$ to $[3.5\ \ 3.5]'$ (see Eq. 18); and d) an off-spec operating was simulated by shifting the average operating point of $\mathbf{t} = [0\ 0]'$ to $\mathbf{t} = [3.2\ \ -1]'$, resulting the average prediction of $\hat{y}_2$ (=2.496) very close to its upper specification limit $y_{2,\max}$(=2.5). The abnormalities were maintained along the following temporal ranges: 11–20, 31–40, 51–60, and 71–80, respectively.

Fig. 5 shows the time evolutions of the combined detection index and its component statistics, and of the inferential quality control index. The alarm condition is triggered at a given sample k, when I_C overpasses the 100(1-α)% confidence (control) limit I_α. As it can be seen, I_C is effective for detecting all simulated abnormalities. The patterns of alarmed component statistics recorded in Fig. 5 allowed an efficient characterization of each fault type and are used to start the diagnosis (Fig. 2). Fig. 6 shows the RBC of $x_1, \ldots, x_7$ to the fault detection index I_C. The contributing variables are clearly identified. In particular, the main contribution of x_1 at $k = 11$ unambiguously identifies the sensor failure. Then, a high value of I_{KX} at $k = 31$ (Fig. 5) together with three significant RBCs (Fig. 6) successfully identify an anomaly of type 3 (as a disturbance, in this case). Finally, a high I_{MX} at $k = 51$ (Fig. 5) successfully identifies an anomaly of type 1, which is an operating point in extrapolation region. In addition, Fig. 5 shows an alarm of off-spec operation during the time interval 71–80, and it is identified by a quality control index $d(\hat{\mathbf{u}}, P)$ greater than zero, while the I_C is in-control.

Notice that the rate $T_{\mathbf{t}}^2/K^2$ (where $T_{\mathbf{t}}^2 = T_{\mathbf{u}}^2$ and K^2 is the multivariate control limit modified by the specifications) is a measure more conservative than $d(\hat{\mathbf{u}}, P)$ for quality control (see the false positive and true positive alarms in Fig. 4b). However, the contributions to the index $T_{\mathbf{t}}^2/K^2$ are useful for determining an appropriate corrective action.

It is important to note that while quality attributes can be correlated, specifications are normally independently imposed. Such practice can potentially result in tolerances that are narrower than acceptable quality ranges. The analyzed process was incapable with a $MC_P = 0.6524$. Then, to get a capability index near of one, Eq. (19) can be used to compute relaxations $\mathbf{s}$ of the original limits, but replacing the last constraints by the followings: $\|\rho\, \boldsymbol{\Delta}^{1/2} \mathbf{a}_i\| \le \mathbf{b}(i) + \mathbf{s}(i)$, $i = 1, \ldots, 2p$. Fig. 7 shows the new effective specifica-

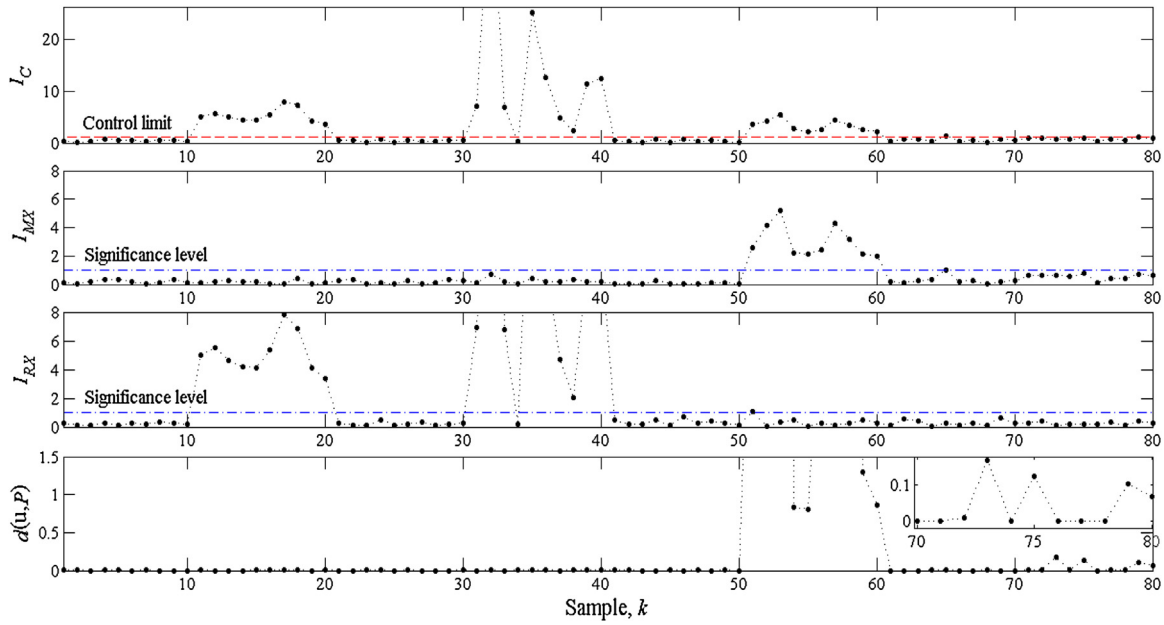

Fig. 5. Time evolutions of: i) the combined detection index I_C; ii) the statistics I_{MX} and I_{RX} that compose I_C (where a significance level of 1 was adopted [11]); and iii) the inferential quality control index (i.e., the distance from incoming **x** to the set *P*).

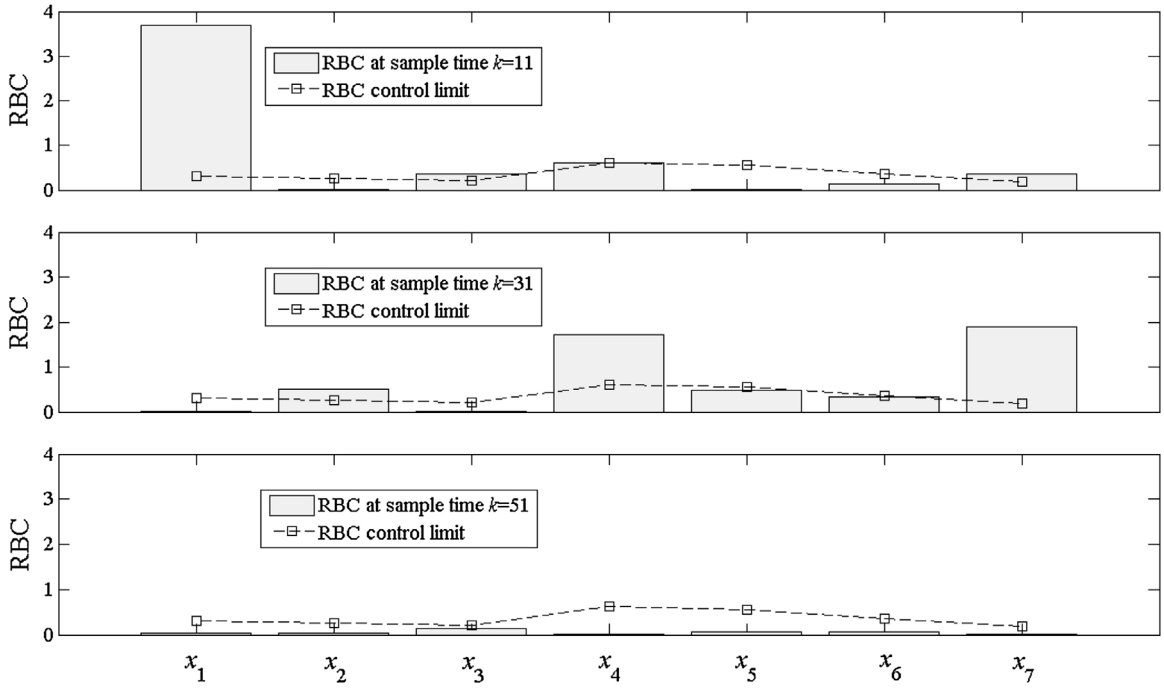

Fig. 6. RBCs of the **x** components in the sample times $k = 11$, 31, and 51.

tion region (i.e. the extended region) with a $MC_P = 1.2795$ and a $\rho^2 = K^2$ density contour.

3.2. Inferential quality control of the industrial SBR process

The industrial Styrene-Butadiene Rubber (SBR) is normally produced through an emulsion polymerization process that is carried out in a train of 7 ~ 15 continuously-stirred tank reactors operated under isothermal conditions. A detailed mathematical model of the SBR polymerization process that was adjusted to reproduce the main process variables recorded in an industrial plant has been published [29]. The model has successfully been used for determining optimal steady-state process conditions [30], for minimizing the off-spec produced between steady-states [31], and for determining global optimization procedures that maximize the rubber production and minimize the transients between steady-states [32]. More recently, Godoy et al. [21] developed a PLS model for representing the same industrial SBR process carried out in a train of 7 operative reactors, and then derived a PLS-based soft-sensor capable of monitoring the main production and quality variables. In this sense, the model of the SBR process has extensively been studied, and therefore we will here assume that such model acceptably represents the industrial process.

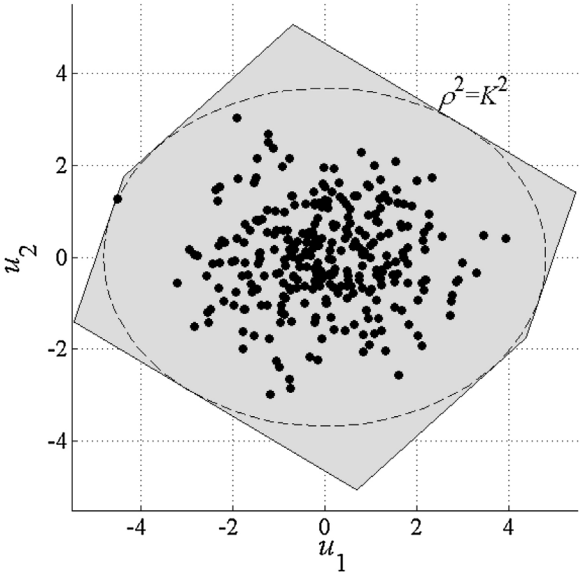

Fig. 7. New effective specification region containing the ρ^2 density contour.

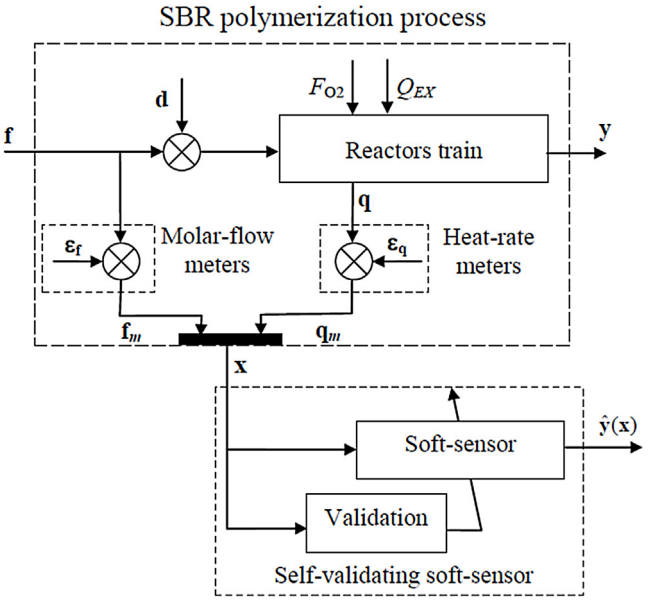

Fig. 8. Quality control in the SBR polymerization process with a self-validating soft-sensor. The soft-sensor predictions ($\hat{\mathbf{y}}$) are confirmed, corrected, or rejected by the proposed validation strategy.

An inferential quality control of the SBR process was simulated based on the PLS model [21]. The following variables were monitored in the last reactor of the train: the mass conversion (x), the solids fraction (x_{sol}); the fraction of styrene linked to the copolymer (p_S), the average particle diameter (d_p), the mass production (G), the number (M_n) and weight (M_w) average molecular weights, and the average number of tri- and tetra-functional branches (B_{n3}, B_{n4}). The upper part of Fig. 8 schematizes the industrial SBR polymerization process, where the output vector at the last reactor of the train is: $\mathbf{y}' = [x, x_{sol}, p_S, d_p, G, M_n, M_w, B_{n3}, B_{n4}]$ (9×1). The prediction $\hat{\mathbf{y}}$ is obtained from the measurement vector $\mathbf{x}' = [\mathbf{f}'_m \; \mathbf{q}'_m]$ (15×1), where $\mathbf{f}_m$ (8×1) contains the molar flow rates of reagents incorporated into the first reactor of the train, while $\mathbf{q}_m$ (7×1) contains the reaction heat rates in each reactor. The measurements are affected by additive random errors, $\boldsymbol{\varepsilon}_f$ and $\boldsymbol{\varepsilon}_q$. Vectors $\mathbf{f}_m$ and $\mathbf{q}_m$ are built as follows: $\mathbf{f}'_m = [F_S, F_B, F_W, F_I, F_{Fe}, F_{RA}, F_E, F_X]$, where the subscripts indicate the reagents: S (styrene), B (butadiene), W (water), I (initiator), Fe (ferrous sulfate), RA (reducing agent), E (emulsifier), and X (chain transfer agent); and $\mathbf{q}'_m = [Q_R^1 \ldots Q_R^7]$, where superscripts indicate the reactor number. The effective flows entering into the first reactor are obtained from the original flows $\mathbf{f}$ disturbed by possible alterations in their purities $\mathbf{d}$. Also, the actual plant can be disturbed by an undesired oxygen inlet (F_{O2}) that acts as an inhibitor of the reaction, and by a varying heat exchange with the environment (Q_{EX}). The presence of such disturbances can clearly turn unreliable the soft-sensor predictions.

Godoy et al. [21] showed that the molar flow rates of the initiation system (F_I, F_{Fe}, and F_{RA}) have negligible effects on the soft-sensor predictions. For this reason, such measurements were excluded from $\mathbf{x}$, which leads to the following optimal input vector: $\mathbf{x} = [\mathbf{f}'_m \; \mathbf{q}'_m]'$ (12×1), with $\mathbf{f}_m = [F_S \, F_B \, F_W \, F_E \, F_{CTA}]'$ (5×1). The three excluded flow rates should be monitored separately in order to supervising their values. The number of latent variables retained in the PLS model was 8. To calculate the control limit K^2, the tolerances of the 9 quality variables at the train output were considered to build the tolerance hypercube in $\Re^9$. Then, $\rho^2 = K^2$ is adopted for this study case.

The sensors considered in this work for measuring molar flow rates of reagents ($\mathbf{f}_m$) and reaction heat rates ($\mathbf{q}_m$) are not included in any closed-loop control strategy. For this reason, any failure originated in those sensors will not affect the operating point. The soft-sensor in Fig. 8 produces a correct prediction in absence of sensor faults, provided that the disturbances ($\mathbf{d}$, F_{O2}, Q_{EX}) are not significant. In fact, type 2 abnormalities do not alter the actual operation of the process, but the predictions are erroneous due to faulty readings in $\mathbf{x}$. This undesired effect is attenuated by means of the reconstruction of $\mathbf{x}$ (Eq. 14). In contrast, the type 3 abnormalities modify $\mathbf{q}_m$ while the measurements of $\mathbf{f}_m$ remain constant. Due to this correlations change, we cannot ensure reliable output estimations, but we can isolate the actual disturbance.

In particular, changes in the purity of the fed reactants (disturbance $\mathbf{d}$) modify only the reaction heat rates $\mathbf{q}_m$ along the reactor train (see Fig. 8). To isolate these abnormalities (Section 2.3.1.2.), the set of known disturbances was obtained by simulating disturbances of 5% in S, B, I, and RA, and 10% in Fe. Also, the faulty samples $\mathbf{x}_i$ are recorded under steady state conditions. Fig. 8 shows the angular location (θ_{mod}, θ_r) of each disturbance sample $\mathbf{x}_i$ in relation to S_{MX} and S_{RX} (see Fig. 3) with its acceptance region (dotted line). Fortunately, a large separation (larger than $2\cos^{-1}\eta$) is obtained between the regions. Note that the sensor faults exhibit $\theta_{\text{mod}} \approx 90°$, because only one measurement is significantly moved away from S_{MX}, and their locations do not overlap with the acceptance regions. The recipe includes RA in excess for a better performance of the initiation process [32]. Thus, disturbances greater than 30% affect the steady-sate performance, and hence its isolation is unimportant. Note that the angular pattern of the disturbance of 5% in RA is inside the normal zone (Fig. 9). Overall, the disturbances $\mathbf{d}$ have different angular locations (θ_{mod}, θ_r) without overlapping either their acceptance regions or the normal zone. Therefore, the proposed method (Eq. 17) is sufficiently specific to isolate the analyzed disturbances.

Fig. 10(a) shows a disturbance d_S that is not detected by the associated reading F_S (see Fig. 10(b)); however, it affects some reaction heat rates (e.g., the $Q_R{}^1$ measurement, Fig. 10(c)). Fig. 10(d) shows that the proposed index successfully isolates the simulated disturbance after the process stabilization. Other simulated disturbances (d_S, d_B, d_I, d_{FE}) have successfully been detected.

Type 1 abnormalities were also simulated to evaluate the performance of the proposed technique for inferential quality control.

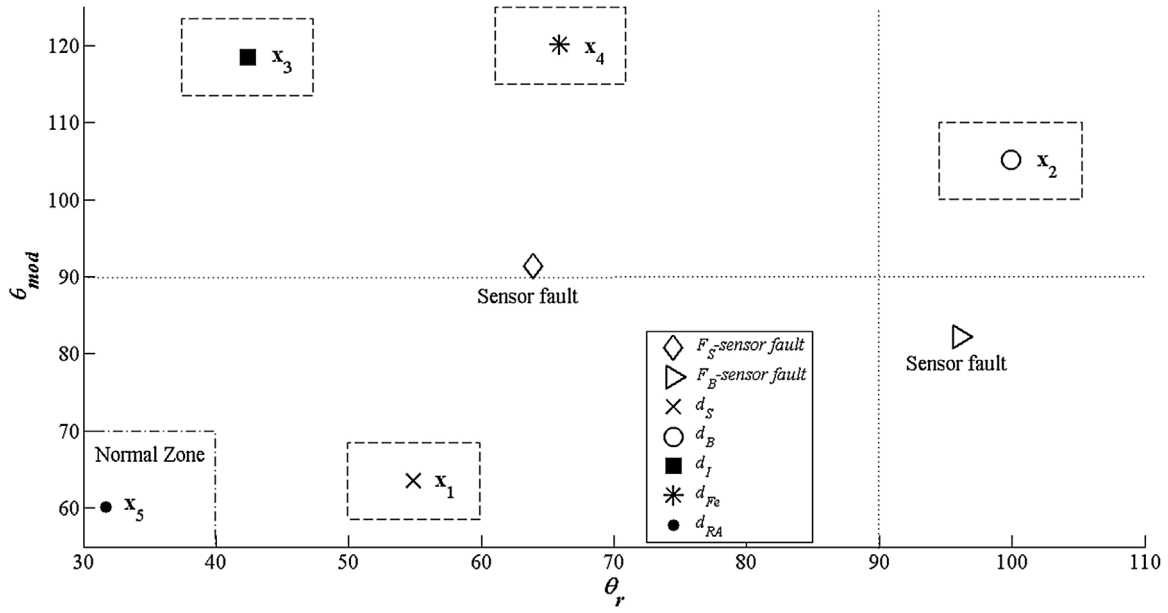

Fig. 9. Angular location (θ_{mod}, θ_r) of the pattern samples $\mathbf{x}_i$ with their individual acceptance regions (subscript $i = \{1,2,3,4,5\}$ corresponds to $\{S, B, I, FE, RA\}$, respectively).

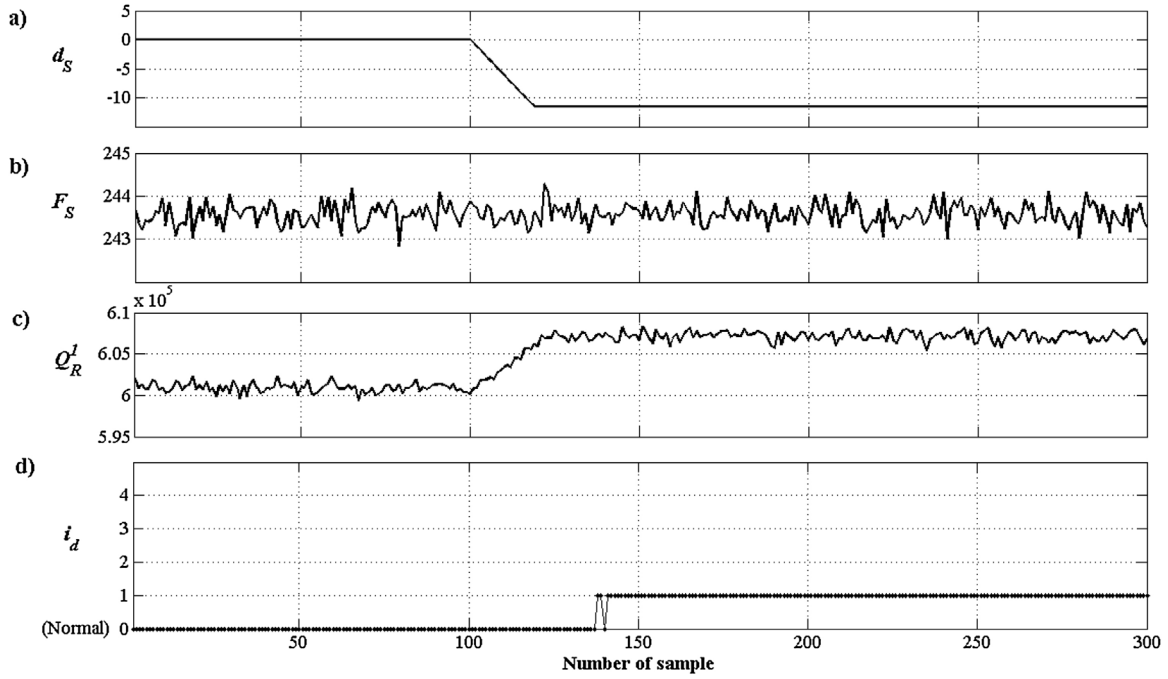

Fig. 10. a) Disturbance in S, d_S. b) Reading of the S-feed flow rate, F_S. c) Reading of the reaction heat rate in the reactor 1, $Q_R{}^1$. d) Time evolution of the isolation index i_d, detecting a disturbance in *S* from the sample time 140, approximately.

To this effect, the operating point of the SBR process was moved to several other operating points that yield off-spec product. In particular, production increments and decrements were simulated by proportionally increasing (or decreasing) the molar flow rates (such practice is not recommended however, because it can yield off-spec product). Although not shown, all the simulated abnormal operating points have been successfully detected and diagnosed.

4. Conclusions

An integral technique for inferential quality control with self-validation of the predictions was presented. The technique uses the PLS model to define an integral design space driven by quality specifications, which is useful to evaluate the impact of both incoming materials and process conditions onto the product quality. Based on this integral design space, a new index for inferential quality control was defined and successfully evaluated. The proposed self-validation strategy uses PLS-decomposition of the measurements for a simultaneous supervision of model extrapolation and process condition through a combined detection index, which includes a multivariate control limit (that depends on the calibration data). This improved self-validation strategy is able to: i) detect and diagnose process faults, ii) automatically correct some particular types of faults, and iii) confirm the estimated variables when no fault is detected or generate an alarm about their unreliability when the detected fault cannot be automatically corrected.

Through numerical simulations, the effectiveness of the technique was successfully evaluated for the quality control of the industrial SBR process. Measurements of reactant flows and reaction heat rates were used as inputs for the inferential control of the main production and quality variables. Flow rate disturbances, sensor faults, and abnormal operations were simulated to test the strategy. All simulated scenarios were adequately detected and diagnosed. The proposed index allows the inferential control of the quality regarding the specifications, in contrast to most techniques that perform control with regard to the variability of historical data. The proposed method is able to isolate feed disturbances and enables the implementation of preventive actions that avoid off-spec products. Therefore, the current PLS strategy might be included in a supervisory control technique of the SBR process, especially when control decisions are deployed infrequently.

Acknowledgements

The authors are grateful for the financial support received from CONICET, MinCyT, Universidad Nacional del Litoral, and Universidad Tecnológica Nacional (Argentina).

References

[1] A. Raich, A. Cinar, Statistical process monitoring and disturbance diagnosis in multivariate continuous processes, AIChE J. 42 (1996) 995–1009.
[2] A. Cinar, A. Palazoglu, F. Kayihan, Chemical Process Performance Evaluation, CRC Press, Boca, Raton, 2007.
[3] H.A.L. Kiers, A.K. Smilde, A comparison of various methods for multivariate regression with highly collinear variables, Stat. Methods Appl. 16 (2007) 193–228.
[4] B. Lin, B. Recke, J.K.H. Knudsen, S.B. Jørgensen, A systematic approach for soft sensor development, Comp. Chem. Eng. 31 (2007) 419–425.
[5] P. Kadlec, B. Gabrys, S. Strandt, Data-driven soft sensors in the process industry, Comp. Chem. Eng. 33 (2009) 795.
[6] J. Gabrielsson, N.-O. Lindberg, T. Lundstedt, Review multivariate methods in pharmaceutical applications, J. Chemom. 16 (2002) 141–160.
[7] S.J. Qin, Survey on data-driven industrial process monitoring and diagnosis, Annu. Rev. Control 36 (2012) 220–234.
[8] J. Liu, D.S. Chen, J.F. Shen, Development of self-Validating soft sensors using fast moving window partial least squares, Ind. Eng. Chem. Res. 49 (2010) 11530–11546.
[9] Y. Masuda, H. Kaneko, K. Funatsu, Multivariate statistical process control method including soft sensors for both early and accurate fault detection, Ind. Eng. Chem. Res. 53 (2014) 8553–8564.
[10] C.F. Alcala, S.J. Qin, Analysis and generalization of fault diagnosis methods for process monitoring, J. Process Control 21 (2011) 322–330.
[11] J.L. Godoy, J.R. Vega, J.L. Marchetti, A fault detection and diagnosis technique for multivariate processes using a PLS-decomposition of the measurement space, Chem. Intell. Lab. Syst. 128 (2013) 25–36.
[12] C.F. Alcala, S.J. Qin, Reconstruction-based contribution for monitoring, Automatica 45 (2009) 1593–1600.
[13] S. Yoon, J.F. MacGregor, Fault diagnosis with multivariate statistical models, part I: using steady state fault signatures, J. Process Control 11 (2001) 387–400.
[14] G. Li, C.F. Alcala, S.J. Qin, D. Zhou, Generalized reconstruction based contributions for fault diagnosis with application to the tennessee eastman process, IEEE Trans. Control Syst. Technol. 19 (2011) 1114–1127.
[15] ICH-Q8, Guidance for Industry: Q8 Pharmaceutical Development, Center for Drug Evaluation and Research, U.S. Food and Drug Administration, Rockville, MD, USA, 2016.
[16] S. Garcia-Munoz, Two novel methods to analyze the combined effect of multiple raw-materials and processing conditions on the product's final attributes: JRPLS and TPLS, Chem. Intell. Lab. Syst. 133 (2014) 49–62.
[17] K. Azari, J. Lauzon-Gauthier, J. Tessier, C. Duchesne, Establishing multivariate specification regions for raw materials using SMB-PLS, IFAC-PapersOnLine 48 (8) (2015) 1132–1137, 9th ADCHEM 2015–IFAC.
[18] J.F. MacGregor, M.J. Bruwer, A framework for the development of design and control spaces, J. Pharm. Innovation 3 (2008) 15–22.
[19] J.R. Richards, J.P. Congalidis, Measurement and, Control of polymerization reactors, Comp. Chem. Eng. 30 (2006) 1447–1463.
[20] J.C. Gonzaga, L.A. Meleiro, C. Kiang, R. Maciel Filho, ANN-based soft-sensor for real-time process monitoring and control of an industrial polymerization process, Comp. Chem. Eng. 33 (2009) 43–49.
[21] J.L. Godoy, R.J. Minari, J.R. Vega, J.L. Marchetti, Multivariate statistical monitoring of an industrial SBR process: soft-sensor for production and rubber quality, Chem. Intell. Lab. Syst. 107 (2011) 258–268.
[22] P. Geladi, B. Kowalski, Partial least-squares regression: a tutorial, Anal. Chim. Acta 185 (1986) 1–17.
[23] A. Höskuldsson, PLS regression methods, J. Chemom. 2 (1988) 211–228.
[24] L. Vandenberghe, S. Boyd, S.P. Wu, Determinant maximization with linear matrix inequality constraints, SIAM J. Matrix Anal. Appl. 19 (1998) 499–533.
[25] C. Beardah, M. Baxter, Matlab Routines for Kernel Density Estimation and the Graphical Representation of Archaeological Data, Tech. rep., Nottingham Trent University Department of Mathematics, Statistics, and Operational Research, UK, 1995.
[26] C. Bishop, Neural Networks for Pattern Recognition, Clarendon Press, Oxford, 1995.
[27] E. Martin, A. Morris, Non-parametric confidence bounds for process performance monitoring charts, J. Process Control 6 (1996) 349–358.
[28] J.L. Godoy, J.R. Vega, J.L. Marchetti, Relationships between PCA and PLS-regression, Chem. Intell. Lab. Syst. 130 (2014) 182–191.
[29] L.M. Gugliotta, M.C. Brandolini, J.R. Vega, E.O. Iturralde, J.L. Azum, G.R. Meira, Dynamic model of a continuous emulsion copolymerization of styrene and butadiene, Polym. React. Eng. 3 (1995) 201–233.
[30] J.R. Vega, L.M. Gugliotta, M.C. Brandolini, G.R. Meira, Steady-State optimization in a continuous emulsion copolymerization of styrene and butadiene, Lat. Am. Appl. Res. 25 (1995) 207–214.
[31] J.R. Vega, L.M. Gugliotta, G.R. Meira, Continuous emulsion polymerization of styrene and butadiene: reduction of off-Spec product between steady-States, Lat. Am. Appl. Res. 25 (1995) 77–82.
[32] R.J. Minari, J.R. Vega, L.M. Gugliotta, G.R. Meira, Continuous emulsion styrene-Butadiene rubber (SBR) process: computer simulation study for increasing production and for reducing transients between steady states, Ind. Eng. Chem. Res. 45 (2006) 245–257.